REVIEW OF MAGNETIC SHIELDING DESIGNS OF LOW-BETA CRYOMODULES

R.E. Laxdal, TRIUMF, Vancouver, Canada

Abstract

It is well known that superconducting cavities can trap magnetic flux while cooling through transition. The trapped flux adds to the residual rf surface resistance. For this reason magnetic shielding is added to the cryomodules to shield the cavities from the environmental magnetic field. The low beta portion of many superconducting hadron linear accelerators, either in operation or in production, includes cryomodules containing one or more high field superconducting solenoids. The operation of a high field solenoid in close proximity to a cavity adds a level of complexity to the cryomodule design considerations. A workshop on magnetic shielding for cryomodules was hosted by MSU in March 2013. The paper will summarize the various techniques that can be employed to reduce the risk of magnetic pollution from internal solenoids and reflect on the workshop.

INTRODUCTION

There has been a renaissance in superconducting hadron linear accelerators (linacs) in the last decade. Upgrades have been completed (ISAC-II [1], IUAC [2]) or are in progress (ATLAS [3]) and several are under development (FRIB [4], IFMIF [5], Project-X [6], RAON [7]) or construction (SPIRAL-II [8]). In the low beta stages of these linacs the transverse momentum with respect to the longitudinal momentum is relatively high so that transverse focussing correction demands are high. Here there are two basic solutions that are considered. In one case room temperature quadrupole doublets are proposed with short cryomodules containing one or more cavities depending on the beam velocity. In the case of the former the magnetic shielding is relatively straightforward since only the external magnetic field need be considered. Existing facilities that opt for this approach are INFN-LNL where they use a combination of sputtered niobium on copper cavities and bulk niobium cavities. Planned projects using this approach are SPIRAL-II and RAON. In the other variant long cryomodules are used with the cavities placed in close proximity to high field superconducting solenoids. Existing facilities that have adopted this approach are ATLAS, ISAC-II, IUAC, SARAF [9] and ReA3 [10]. Planned facilities that will use this approach are IFMIF [see Fig. 1], FRIB, Project-X, C-ADS [11] and Beijing-ISOL [12]. In the second variant the superconducting solenoids exist in close proximity to the cavities and a host of possible magnetic contaminations must be considered.

In March 2013 FRIB hosted a workshop on Magnetic Shielding for Cryomodules. Participants from FNAL, TRIUMF, CEA, KEK, INFN-LNL as well as FRIB took part in the two day exchange. This paper in part is a summary of the highlights of the presentations and discussions.

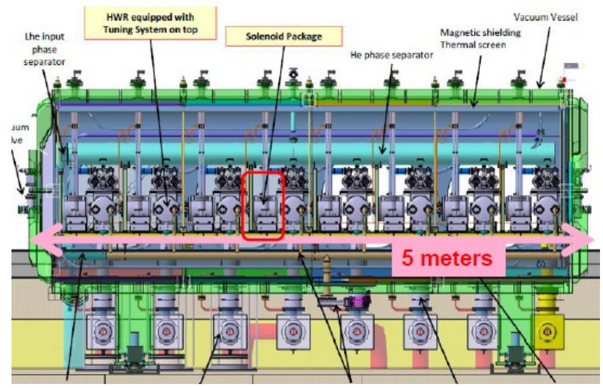

Figure 1: IFMIF cryomodule with 8 HWR and 8 solenoids in an alternating lattice.

MAGNETIC FIELD POLLUTION

When cooled below transition to a temperature $T<T_c$ and with a background magnetic field $H<H_{c1}(\mathrm{T})$ a theoretical Type II superconductor should reside in the Meissner state, the material should be perfectly diamagnetic and the magnetic field should be completely rejected from the SC volume. However surface defects weaken the Meissner state and become a source for pinning centers that trap flux during cooldown. It is found that `cavity quality' bulk niobium in the presence of a low residual field will trap 100% of the flux[13]. The field enters the bulk as fluxoids surrounded by current vortices with normal cores. RF currents see these normal areas as loss sites that increase the rf surface resistance with an approximate value given by the normal surface resistance and the fraction of the surface that is normal [14]

$$R_m = \frac{H_{ext}}{H_{c2}} R_n \text{ with } R_n = \sqrt{\frac{\omega \mu_0}{2 \cdot RRR \cdot \sigma}}$$

where R_m is the contribution to the residual surface resistance due to trapped flux, H_{ext} is the background field present during transition crossing and R_n is the normal surface resistance of the material at the operating temperature assuming the non-anomalous case. This gives the sensitivity of surface resistance to trapped flux as

$$\frac{R_m}{H_{ext}} = \frac{1}{H_{c2}} \sqrt{\frac{\omega \mu_0}{2\sigma \cdot \mathrm{RRR}}} .$$

Note that the sensitivity of the surface resistance due to trapped flux is inversely dependent on H_{c2} so that sputtered niobium films where H_{c2}~30000 are somewhat

ISBN 978-3-95450-143-4

less sensitive than bulk niobium films. For bulk niobium with RRR=300, H_{c2}=4000, σ=6.6x10^{-6} the sensitivity is 3.5 nΩ/μT at 1 GHz though this factor is dependent on the surface treatment [15]. For low beta cavities with frequencies near 0.1GHz the sensitivity is moderated to 1.1 nΩ/μT.

The specification for a given project is dependent on the operating parameters and the quality of the cavity fabrication and processing. The active cryogenic load is directly related to the surface resistance which is given by

$$R_s = R_{BCS} + R_0 + R_m .$$

Where R_{BCS} is the BCS surface resistance and for RRR=300 niobium is approximated by

$$R_{BCS}[\mathrm{n}\Omega] \approx 2\times10^5 \frac{1}{T}\left(\frac{f[\mathrm{GHz}]}{1.5}\right)^2 \exp\left(-\frac{17.7}{T}\right)$$

and R_0 is the residual resistance reflective of the cavity quality.

To date low beta systems have operated at 4 K and high beta at 1.8 or 2 K with R_{BCS} in the range of 5-10 nΩ and residual resistances for good cavities in the same range. Here a specification of R_m<~3 nΩ seems appropriate resulting in a tolerance of H_{ext} < 1 - 3 μT for frequencies ranging from 1 GHz to 0.1 GHz respectively. A plot comparing R_{BCS} and R_{mag} as a function of frequency assuming different background fields is shown in Fig. 2. A recent trend is to design large cw low – medium beta linear accelerators to operate at 2 K to reduce the Q-slope [4]. In this case R_{BCS}<1 nΩ for f<400 MHz and Q-slope is markedly reduced so that an operating rf surface resistance in the 5 nΩ range is plausible. In this case it is worthwhile to further tighten the magnetic field specification to R_m<~1 nΩ resulting in a tolerance of H_{ext} < 0.3 - 1 μT for frequencies ranging from 1 GHz to 0.1 GHz respectively.

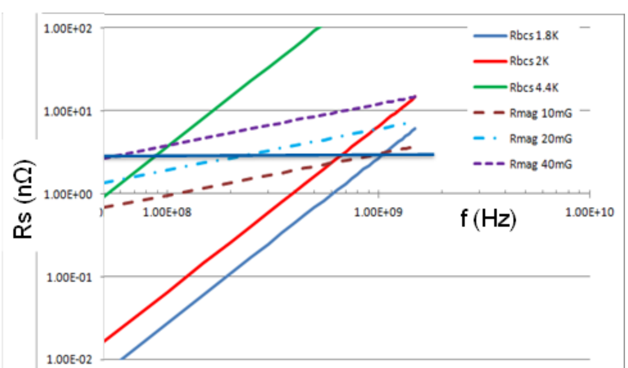

Figure 2: BCS and magnetic contributions to the RF surface resistance as a function of rf frequency for different temperatures and background fields.

SHIELDING THE EXTERNAL FIELD

The earth's magnetic field is typically 50 μT. Based on the field tolerance discussion a suppression of ~20-100 would be required. Here there are two basic variants – the global shield and the local shield (see Fig. 3). In the global shield a high permeability Nickel alloy `mu-metal' sheet is used usually just inside the vacuum chamber to shunt the external field and suppress the magnetic field in the internal cryomodule space. The positive feature of the approach is the simplicity. The mu-metal operates in a warm state and can be prepared in a straightforward way to match the openings in the vacuum wall. In general openings should be kept small and seams should be overlapped to maximize the performance. In the local shield variant a mu-metal that is annealed for cold service is fitted in close proximity to the cavity or cavities. The shield is more complex to design and fabricate since all the cavity ports and supports plus external shape have to be taken into account. The positive side is that the shield is much smaller, and therefore will intercept less flux and is less prone to saturate. Another potential advantage to the shield is that the fringe field from the solenoid can be shielded from the cavity while in the global shield only the external field is suppressed.

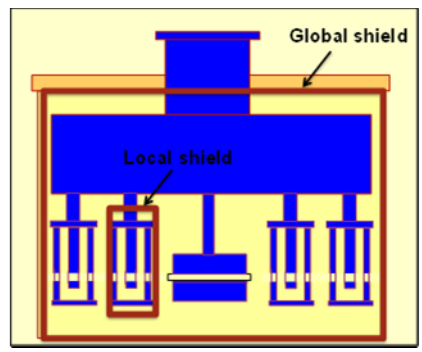

Figure 3: Global vs local shield in a low beta cryomodule.

POLLUTION FROM THE SOLENOID

Imagine a high field (9 T) solenoid operating inside a superconducting rf cryomodule (Fig. 4). The solenoid can potentially affect the cavity performance in a few ways. When cold the cavity is in the Meissner state the external wall of the cavity will repel the field of the solenoid and the rf surface will be unaffected as long as the fringe field is much smaller than H_{c1}, ~160 mT. The fringe field from a strong solenoid however can pollute the environment inside the cryomodule. Components in the cryomodule, including mu-metal, that can be magnetized will be magnetized by the solenoid fringe field. As long as the cavity is in the Meissner state the cavity performance will be unaffected. However if the cavities warm above

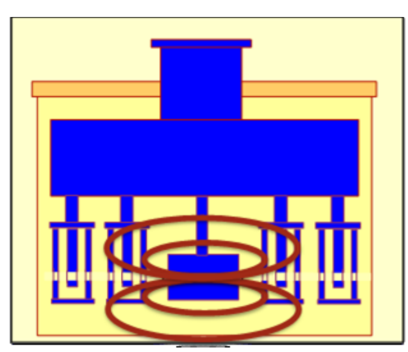

Figure 4: Schematic of fringe field from a solenoid.

ISBN 978-3-95450-143-4

transition either by design or during a cryogenic event the excess residual field from the local magnetization will be trapped by the cavity and will increase the surface resistance. Further the solenoid can be the source of its own flux due to flux pinned in the conductor matrix so that even when the current is zeroed it is still a source of internal magnetic field. The solenoid fringe field can also pollute the cavity if the cavity experiences an rf quench. In this case the stored energy of the cavity dissipates in the quench location and warms up the cavity wall around the quench location. The heating causes a `normal hole' to open (see Fig. 5) that allows the fringe field to enter the niobium. The wall will quickly cool after the rf is extinguished but the `normal hole' will trap the ambient flux and increase the power dissipation in the normal zone and lower the Q by

$$P_q = \frac{1}{2} A_q H_q{}^2 R_{mq} \text{ and } Q = \frac{V^2}{R/Q\left(P_c + P_q\right)}$$

where P_q is the rf power absorbed in the quench hole after cooldown, A_q is the area of the normal hole, H_q is the rf field at the quench location, R_{mq} is the surface resistance due to the magnetic pollution at the quench zone.

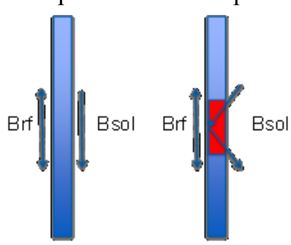

Figure 5: Schematic of a quench where the cavity wall warms above transition and the solenoid fringe field penetrates the niobium and is trapped on cooldown.

Mitigation Strategies

To avoid magnetization of the environment in an unshielded solenoid the materials used in close proximity to the solenoid and cavity should be chosen carefully from material that is not easily magnetized. Stainless steel 316LN is a good choice although even this material can become susceptible to magnetization after welding or cold working. Attention should be paid to hardware including bolts and nuts, bearings and diagnostics.

The cavity can be rendered somewhat insensitive to the internal environment if a local magnetic shield is used. In this case the remnant field from the solenoid is shunted around the cavity during solenoid operation and after warm-up. The concern here would be that the mu-metal itself would become magnetized and degrade the cavity performance on the subsequent cooldown. The shield is first modelled with a 3-D rendering code that fits the shield around the cavity and interface interferences. Once fabricated the formed shield is given a final anneal.

The solenoid can be isolated from the environment by adding an iron return yoke to reduce the fringe field and/or containing the solenoid in an outer shield. The danger is that the solenoid shield will become magnetized to an extent that it cannot be perfectly degaussed.

A final solution is the minimalist approach. In this case the cryomodule is initiated as an unpolluted environment by correct choice of material and with a good global shield and the solenoid is used to erase magnet memory by employing a degaussing cycle before every warm-up.

MAGNETIC SHIELD WORKSHOP (FRIB)

A magnetic shielding workshop was held at FRIB in March 2013. The workshop hosted 11 external attendees from TRIUMF, CEA, FNAL, INFN-LNL, KEK, Amuneal, plus FRIB participants. Topics included:

- Degaussing studies
- Global vs local shielding
- Solenoid design issues
- Q degradation during quench
- Magnetic shielding materials characterization

Degaussing Studies

In ISAC-II the magnetic shielding approach adopts a minimalist strategy [15]. ISAC-II has adopted non-magnetic materials where possible with no shielding between the cavity and solenoid. Instead procedures are used to provide adequate field suppression to support operation.

In this case a degaussing of the solenoid is essential before any planned warm-up to erase magnet memory. For example during cryogenic events (1-2 per year) of more than a few hours the cavities with a relatively small thermal mass can warm above transition. In this case the solenoid is degaussed and then heated above transition to release frozen flux by an internal heater. The procedure takes 30 minutes to degauss and 30 minutes to warm to ~25 K and a further 60 minutes to cool everything down. It should be noted that the cavities are insensitive to quench degradation since they have a reactor grade jacket which acts as an external Meissner shield. During the commissioning of the ISAC-II cryomodules data was taken comparing the remnant field in the cryostat with and without a degaussing cycle after energizing the solenoid [16]. The data, summarized in Fig. 6, records the remnant field in the cryomodule both before and after driving the solenoid to full current corresponding to 9 T. All data is take with the cryomodule warmed and vented. The remnant field is increased from ~2-3 µT to more than 10 µT by magnetization from the solenoid. Later the remnant field is reduced through a degaussing cycle as indicated by the third survey.

The TRIUMF degaussing recipe is to drive the solenoid in the opposite polarity to 1.3 times the operating level and then to continue driving the solenoid in opposite polarities with 75% of the previous field until the smallest step of the solenoid supply.

In the case of the ANL cryomodule development a solenoid was placed in close proximity to an ANL tapered QWR for degaussing studies [17]. In this case the measured fields at the cavity flange (Fig. 7) were successfully reduced below 1 µT by employing a degaussing cycle after powering the solenoid to 6 T.

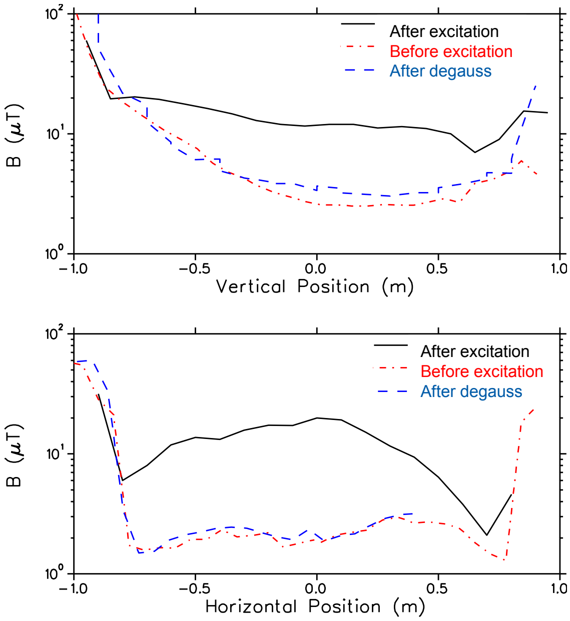

Figure 6: Internal magnetic residual field for vertical and horizontal scan before and after solenoid excitation to 9T and then after a degaussing cycle.

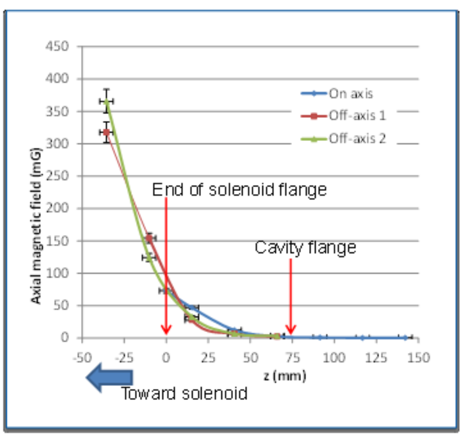

Figure 7: Fringe field as a function of distance from the solenoid after powering to 6 T and degaussing.

In the case of FRIB a TDCM (technical demonstration cryomodule) was designed and assembled to test aspects of the FRIB cryomodule design. The device houses both a solenoid and superconducting cavities as well as various diagnostics. With regard to degaussing studies cavity performance first indicated that magnetic pollution did significantly degrade cavity performance and later a degaussing step did confirm that the remnant field could be erased to less than 1 μT at the cavity (Fig. 8)[18]. In the case of FRIB the current is ramped in bipolar fashion, at ±I, ±0.8I, ±0.64I, to the smallest current increment.

Global vs Local Shielding

To date most of the superconducting heavy ion linacs (ISAC-II, ANL, LNL, SARAF) have chosen global magnetic shields of from 1 to 1.5 mm in thickness. An exception is the SPIRAL-II high beta cryomodules where

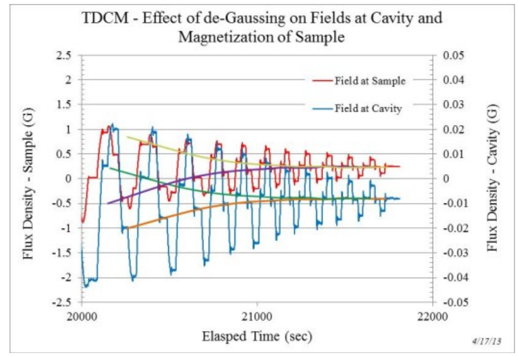

Figure 8: Degaussing effect at a sensor near the cavity and in a sensor in a magnetized SS sample.

cold mu-metal is chosen in close fit around each cavity. In the case of projects in the design stage recent studies have been done at FRIB, CEA and TRIUMF. At FRIB for the QWR cryomodule a specification of B<1.5 μT has been adopted. In this case simulation studies indicate that due to the length of the module a shielding thickness of 3mm is required. For comparison a cold local shield of 1 mm wall thickness is sufficient to meet the specification. Both single cavity and multiple cavity cold shields are employed (Fig. 9).

The local shield also helps to reduce some of the requirements on cryomodule parts by partially shielding the internal magnetic pollution due to magnetization from the solenoid. FRIB's conclusion is that local shielding can be cheaper, easier to handle/assemble, and relaxes requirements on screening magnetizable components before assembly.

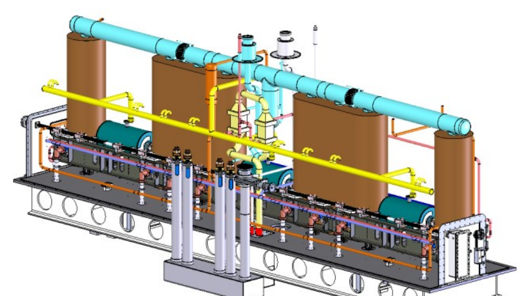

Figure 9: FRIB low beta cryomodule showing local magnetic shield around cavities.

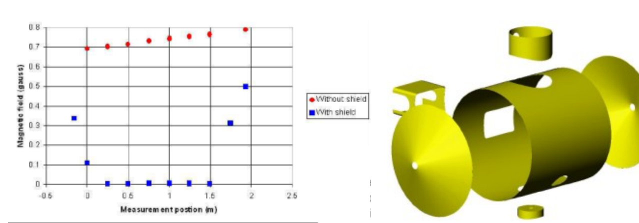

Figure 10: FNAL horizontal test cryostat shielding and field mapping data showing suppressions of >70.

ISBN 978-3-95450-143-4

FNAL reported on their experience with their horizontal test cryostat where a 1.5 mm thick custom shield has been designed, fabricated, installed and tested. For the 1.2 m diameter vessel a shield of 1.5 mm thick mu-metal was chosen and achieved a remnant field of < 1 µT for a total suppression >70 (see Fig. 10).

Based on this experience FNAL has chosen a 1.5mm thick global shield for their 325 MHz SSR1 cryomodule for Project X with a specified B< 1 µT.

CEA Saclay is working on a number of different cryomodule projects including ESS, XFEL, SPIRAL-II (low beta CM) and IFMIF. For the IFMIF demonstrator cryomodule with 8 HWR and 8 solenoids on-board they have chosen a 1mm global shield. For the SPIRAL-II low beta cryomodule they have chosen a 1mm thick global shield with a measured attenuation of >50. For ESS and XFEL a local cold shield is adopted with a thickness of 1.5mm and 1mm respectively. In particular for XFEL magnetic measurements confirm that the iron vacuum vessel is responsible for an attenuation of a factor of 5 while the cold mu-metal reduces the remnant field by a further factor of 25 for a total attenuation of >100 (Fig. 11).

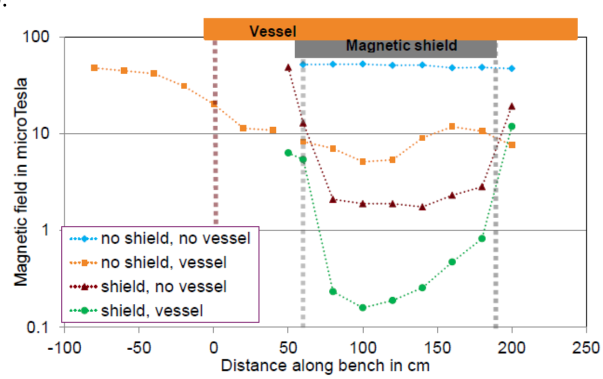

Figure 11: Measured field for the XFEL vacuum vessel and local cavity shield for different configurations.

For ARIEL the magnetic field suppression has been tested with an active background provided by a Helmholtz coil that can increase the ambient field from ~30 µT to ±500 µT. The active field can also be used to cancel a uniform background field. Two layers of mu-metal – a 1 mm global shield and a 1 mm local shield are employed in the ARIEL cryomodule [19]. The global shield shows signs of saturation as the background field increases above ambient. Suppression factors of 10 were achieved by the global shield, while the local shield provides suppression factors of a further 50-100 for a measured field of ~0.1 µT for no additional background field and 0.5 µT for a background field of 300 µT (Fig. 12).

Solenoid Design

In ISAC-II focusing in the SC Linac is provided by superconducting solenoids (B≤9 T) with the end fringe fields controlled with active `bucking' coils to a field level of B_{cavity}≤30 mT. A field map of the ISAC-II solenoid at zero current (Fig. 13) has been done for three

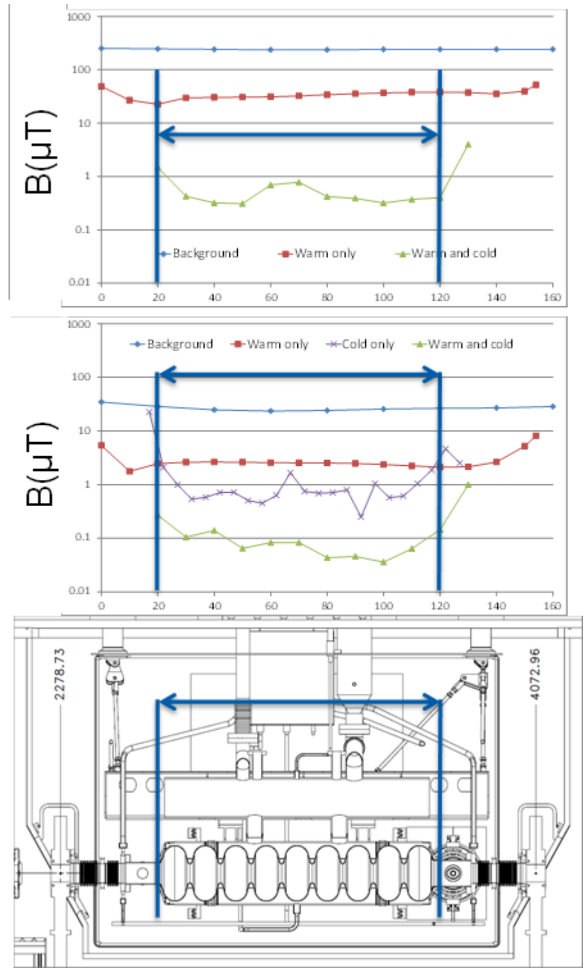

Figure 12: Magnetic field survey of ARIEL injector module (bottom) for a background field of 300 µT (top) and ~30 µT (middle).

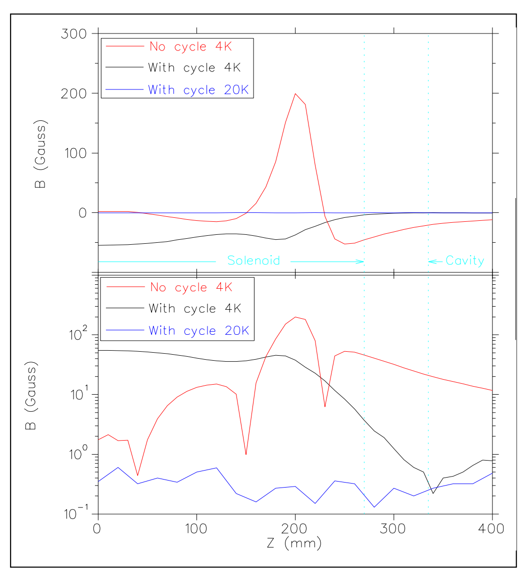

Figure 13: A field map of the ISAC-II solenoid at zero current for three cases: 1) at 4 K with no degauss 2) at 4 K after degauss 3) at 20 K after degauss.

cases: 1) at 4 K with no degauss 2) at 4 K after degauss 3) at 20 K after degauss. The results [16] show that a degauss of the magnet is essential and to truly zero the field a warm-up the coil is required to zero the frozen flux.

The IFMIF prototype cryomodule has 8 HWR and 8 solenoids with each solenoid including a cold BPM and x-y steerers. The specification for the fringe field is <20 mT at the cavity. Both iron shields and active compensation have been considered but iron shields were abandoned due to concerns about remnant field after solenoid excitation. The compensating coil is an external solenoid in series with the main coil (Fig. 14).

FRIB has modeled the solenoid fringe field assuming a local shield around the cavity. The specification is to keep the field at the shield B_{Shield}< 65 mT to avoid saturation of the mu-metal shield. Three cases were looked at: (a) no compensation with B_{Shield}~100 mT (b) active compensation B_{Shield} < 8 mT and (c) passive compensation (iron yoke) with B_{Shield} < 15 mT. Based on this analysis they have chosen the iron yoke variant due to the reduced cost. Further tests are planned in a cryomodule environment.

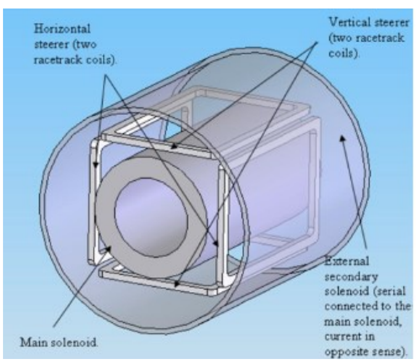

Figure 14: Conceptual design of the IFMIF demonstration cryomodule solenoid.

Q Degradation During Quench

Studies of Q degradation from cavity quenching in the presence of an external field have been done at FNAL and FRIB. In the studies at FNAL three separate cavity tests were completed - two with an elliptical cavity (1.3 GHz and 650 MHz) and one with a spoke cavity. We summarize here results from two of the tests [20-22] with the test configurations shown in Fig. 15. In the first study a 1.3GHz cavity with a known quench location was installed in a vertical test configuration with a solenoid installed in the bath near the quench location – the cavity was quenched at various solenoid field strengths and the cavity Q was measured after each case. In the spoke cavity tests a 325 MHz spoke cavity was placed near a solenoid and resistive heaters were placed at various locations to initiate quenches with a pulse of heat from the bath side – the Q of the cavity was measured as a function of the solenoid field and the position of the quench. A model was developed linking the reduction in Q and the fringe field from the magnet based on an estimation of the size of the `normal opening' in the cavity wall during the quench.

A procedure for `annealing' the quench zone trapped flux was developed by repeated quenching of the zone in the presence of no field. Each quench opened the `normal zone' and allowed the niobium to release the trapped flux. The results of one set of measurements with the 325 MHz SSR1 cavity are shown in Fig. 16. Here the cavity Q values are plotted after quenching the cavity with a solenoid field excited at various currents. Also shown is the Q value after a set of quenches with the solenoid off help to release the flux - `quench annealing'. FNAL developed a model that can fit the results and can be extended to other geometries. Using the trapped flux criterion FNAL decided not to use an iron yoke in the solenoid.

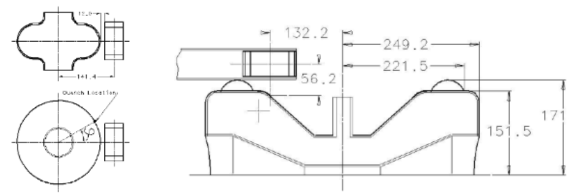

Figure 15: FNAL geometries for the quench tests of the 1.3 GHz elliptical cavity and the 325 MHz spoke cavity. Shown are the cavity and the position of the solenoid.

In the case of the FRIB studies a solenoid is positioned in the high field region of a HWR cavity with a known quench location. The cavity is quenched in the presence of the solenoid field where the field at the cavity is estimated at B (G) ~ I(A)/2 where I is the current in the solenoid. The quality factor of the cavity is monitored as a function of solenoid current. Each time the cavity is also quenched with the solenoid off to release the trapped flux and restore the Q. In this experiment no degaussing step is used between cycles. Fig. 17 shows a particular case with Q curves measured before and after quenching and after a `quench annealing' cycle. A summary of all cases with Q at the expected operating gradient for quenching in the presence of increasing solenoid strength is given in Fig. 18. Quench annealed results are also shown.

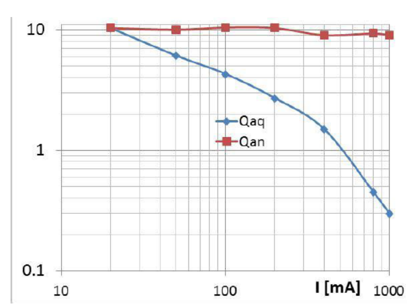

Figure 16: Cavity Q_{aq}x10^{-9} (blue) as a function of excitation current for flux trapping experiments with the 325 MHz SSR1 spoke resonator at FNAL. Also shown is Q_{an} after quench `annealing'.

ISBN 978-3-95450-143-4

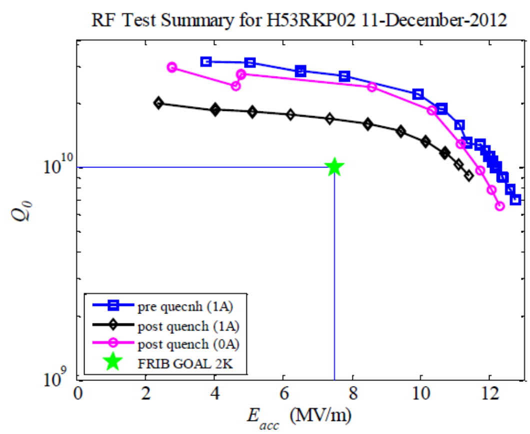

Figure 17: FRIB cavity test results before (blue) and after (black) quenching of a HWR in the presence of a solenoid excited to 1 A (~0.5 G). The pink curve is after a quench with the solenoid off.

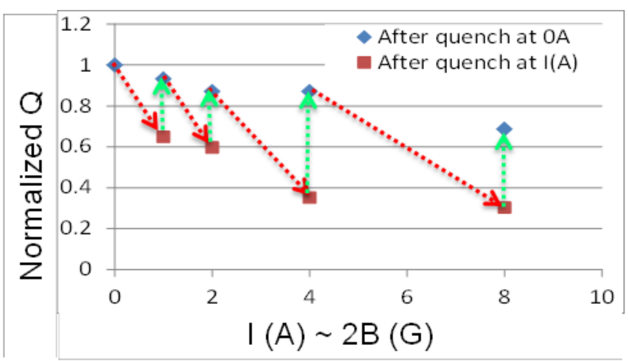

Figure 18: FRIB results with a HWR showing relative Q as a function of solenoid excitation for quenching with solenoid on and quenching with solenoid off.

Shielding Materials

Several laboratories are engaged in qualifying the performance of magnetic shielding material for both warm and cold application. In general the shielding material is a nickel alloy with a special anneal cycle to deliver a high permeability. Studies reveal that in general the standard catalog temperature dependence of permeability for the special cryogenic application materials CRYOPERM and CRYOPHI are not consistent with the measurements. Specifically the thermal performance is not peaked towards low temperatures but is highest at room temperature and gradually declines to cold temperature with less slope than standard mu metal material. Recent data from Amuneal comparing Cryoperm and A4K is presented in Fig. 19. Since the material is very sensitive to the final anneal it is also sensitive to handling. The results of an Amuneal study showing the sensitivity of the material to dropping is given in Fig. 20. In the study the height of the drop and the number of drop cycles are varied. Care should be taken not to shock the mu-metal after final anneal.

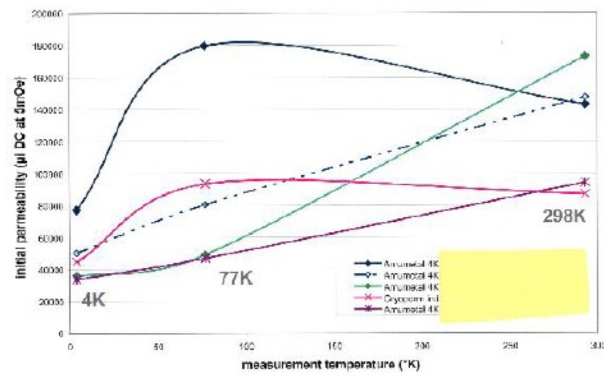

Figure 19: DC permeability for different preparations.

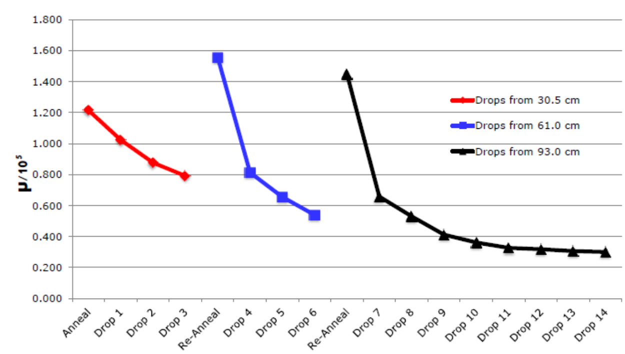

Figure 20: Amuneal data showing the sensitivity of the magnetic permeability of mu-metal to `drops' as a function of height.

KEK and CEA have opened collaboration on magnetic material characterization as part of the France Japan Particle Physics Laboratory Collaboration. The goals of the collaboration are to (1) Measure permeability of many samples to estimate statistical fluctuations from the same lot at various temperatures, (2) Measure permeability of the same sample at CEA and KEK at room temperature and cryogenic temperature to evaluate possible systematic errors between the two groups, (3) further investigate possible causes for the performance degradation of the shielding material at the cryogenic temperature, (4) develop a quality control method, suitable for use in mass production. Data from the collaboration are shown in Fig. 21 for three different materials at three different temperatures.

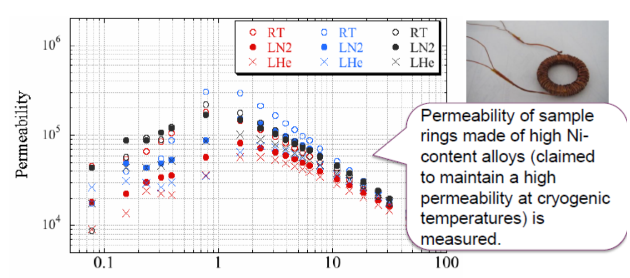

Figure 21: Magnetic permeability data at 300 K, 77 K and 4 K for three different materials.

Permeability of two types of materials were measured at room temperature as a function of strain. The degree of strain is evaluated by parameter, ε, defined as $\varepsilon = e/2R$, where e and R are the thickness of the sample and the radius of the curvature of the forming die, respectively. A significant decrease in permeability due to deformation is measured as summarized in Fig. 22.

FRIB has also set up a program to measure magnetic parameters of materials and mu-metal. Material investigations at room and cryogenic temperature are on-going including characterization of shielding effectiveness, shielding magnetization, and de-Gaussing procedures for mu-metal. In addition realistic shield designs will be tested for saturation point and attenuation.

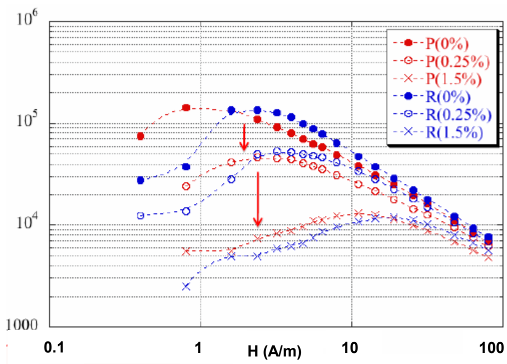

Figure 22: Permeability as a function of applied field for two different materials at three levels of strain.

ACKNOWLEDGMENTS

Thanks to Kenji Saito of FRIB for organizing the magnetic shielding workshop and to the participants for all the information. Additional information was provided by Mike Kelly and Sanghoon Kim of ATLAS, Joe Ozelis of FRIB, Dan Berkovits of SARAF and Prakash Potukuchi of IUAC.

REFERENCES

[1] R. Laxdal, et al., `Operating Experience of the 20 MV Upgrade Linac', LINAC2010, Tskuba, Sept. 2010.

[2] A. Roy, `Superconducting Linac and Associated Developments at IUAC Delhi', LINAC2012, Tel Aviv, Sept. 2012.

[3] P. Ostroumov, et al., `Efficiency and Intensity Upgrade of the ATLAS Facility', LINAC2010, Tsukuba, Sept. 2010.

[4] J. Wei, et al., `FRIB Accelerator Status and Challenges', LINAC2012, Tel Aviv, Sept. 2012.

[5] A. Mosnier, `Status of the IFMIF-EVEDA 9 MeV 125 mA Deuteron Linac', LINAC2012, Tel Aviv, Sept. 2012.

[6] N. Solyak, et al., `Design of the Project X CW Linac, LINAC2010', Tsukuba, Sept. 2010.

[7] D. Jeon, et al., `Status of the RAON Accelerator Systems', IPAC2013, Shanghai, June, 2013.

[8] R. Ferdinand, et al., `The SPIRAL 2 Superconducting Linac', LINAC2008, Victoria, Sept. 2008.

[9] D. Berkovits, et al., `Operational Experience and Future Goals of the SARAF Linac at SOREQ', LINAC2012, Tel Aviv, Sept. 2012.

[10] O. Kester, et al., ReA3 - the Rare Isotope Re-accelerator at MSU, LINAC2010, Tsukuba, Sept. 2010.

[11] Y.L. Chi, et al., `Chinese ADS Project and Proton Accelerator Development', LINAC2012, Tel Aviv, Sept. 2012.

[12] W. Liu, Nucl. Phys. News 22, 29 (2012).

[13] S. Aull, et al., `Study of Trapped Magnetic Flux in Superconducting Niobium Samples', SFR2011, Chicago, Sept. 2011.

[14] H. Safa, `Surface Effects in SC RF Cavity', CAS - CERN Accelerator School on Superconductivity and Cryogenics for Accelerators and Detectors, Erice, Italy, 8 - 17 May 2002, pp.196-211.

[15] G. Ciovati and A. Gurevich, 2008 Phys. Rev. Special Topics – Accelerators and Beams (PRST-AB), 11122001.

[16] R.E. Laxdal, et al., `Magnetic Field Studies in the ISAC-II Cryomodule', Physica C 441 (2006) 225-228.

[17] S. Kim, private communication.

[18] J. Ozelis, private communication.

[19] R.E. Laxdal, et al., `The Injector Cryomodule for the ARIEL e-Linac at TRIUMF', LINAC2012, Tel Aviv, Sept. 2012.

[20] I. Terechline, `Modeling Quench Propagation in Superconducting Cavity Using COMSOL', FNAL Note TD-11-019.

[21] T. Khabiboulline, et al., `Superconducting Cavity Quenching in the Presence of Magnetic Field', FNAL Note TD-11-020.

[22] T. Khabiboulline, et al., `SSR1 Cavity Quenching in the Presence of Magnetic Field', FNAL Note TD-12-007.

ISBN 978-3-95450-143-4